

Atom Transfer Radical Copolymerization of Hydroxyethyl Methacrylate and Dimethylaminoethyl Methacrylate in Polar Solvents

Raymond L. Teoh, Kyle B. Guice, and Yueh-Lin Loo*

Department of Chemical Engineering, Center for Nano- and Molecular Science and Technology (CNM), University of Texas at Austin, 1 University Station, C0400, Austin, Texas 78712

Received July 21, 2006; Revised Manuscript Received October 5, 2006

ABSTRACT: We determined the reactivity ratios of hydroxyethyl methacrylate (HEMA) and dimethylaminoethyl methacrylate (DMAEMA) during atom transfer radical copolymerization (ATRP) in isopropyl alcohol, tetrahydrofuran, acetonitrile, and dimethyl sulfoxide (DMSO). The reactivity ratios in DMSO are near unity ($r_{\text{HEMA}} = 1.08$ and $r_{\text{DMAEMA}} = 1.12$). While there was considerable deviation between the initial monomer composition and the average polymer composition during copolymerization in most solvents, copolymerization in DMSO resulted in random copolymers of poly(HEMA-*co*-DMAEMA) with average polymer compositions that were identical to the monomer feed compositions. Poly(HEMA-*co*-DMAEMA) copolymers with molar feed compositions of $f_{\text{HEMA}}^0 = 0.25$ and $f_{\text{HEMA}}^0 = 0.50$ were synthesized in DMSO by ATRP with uniform compositions along the polymer chain. These polymers achieve their target molecular weights and are near monodisperse ($M_w/M_n < 1.11$). The glass transition temperatures of these copolymers increase with increasing HEMA content.

Introduction

Poly(hydroxyethyl methacrylate), poly(HEMA), and poly(dimethylaminoethyl methacrylate), poly(DMAEMA), are two functional polymers with widespread applications in areas requiring biocompatibility, such as hydrogels,¹ contact lenses,² and drug delivery systems.³ Poly(HEMA) contains pendant hydroxyl functionalities that render it hydrophilic. Poly(DMAEMA) contains pendant tertiary amines that are easily protonated below its pK_a of 7.5,⁴ thus affording the polymer pH-tunability for controlled-release applications.

Several researchers have sought to combine the hydrophilicity of poly(HEMA) with the pH-responsiveness of poly(DMAEMA).^{1,5} Bulk free-radical copolymerization of HEMA and DMAEMA in the presence of a cross-linking agent results in cationic hydrogel networks with the extent of swelling controlled by changes in pH.^{1,6} These smart materials have thus been used in applications of tissue growth¹ and controlled drug delivery.⁵ While the utility of combining the attributes of HEMA and DMAEMA has been demonstrated, these materials are inherently heterogeneous in cross-link density and comonomer distribution⁷ due to large differences in monomer reactivity.⁸

The distribution of monomers in a polymer chain is related to the reactivity ratios of the comonomers. These reactivity ratios describe the probability with which each monomer is added to the growing polymer chains with respect to that of the other monomer. Ideally, the reactivity ratios of both monomers are unity, in which case the polymer composition at any point during the copolymerization is equivalent to the monomer feed composition. The terminal-model reactivity ratios of HEMA and DMAEMA have been reported for bulk copolymerization ($r_{\text{HEMA}} = 1.63$; $r_{\text{DMAEMA}} = 0.45$),⁸ as well as for copolymerization in water ($r_{\text{HEMA}} = 1.32$; $r_{\text{DMAEMA}} = 0.78$)⁹ and in *N,N*-dimethylformamide (DMF; $r_{\text{HEMA}} = 0.75$; $r_{\text{DMAEMA}} = 0.36$).⁹ In bulk copolymerization and copolymerization in water, $r_{\text{HEMA}} > 1$ while $r_{\text{DMAEMA}} < 1$. Correspondingly, the addition of HEMA monomer to the growing chain is more probable than the addition of DMAEMA. This scenario results in considerable

deviation between the monomer feed composition (f_{HEMA}^0) and the instantaneous composition in the copolymer (F_{HEMA}). Even when the copolymerizations are carried out to low and moderate conversions, drifts in the average polymer composition (\bar{F}_{HEMA}) are expected due to the different extents of depletion of the two monomers. It is therefore difficult to maintain compositional homogeneity throughout the copolymerization of HEMA and DMAEMA in the bulk and in water without continuously monitoring and maintaining the instantaneous monomer composition (f_{HEMA}) during the reaction. As a consequence, the resulting copolymers are initially enhanced in HEMA and enriched in DMAEMA in the tail. On the other hand, r_{HEMA} and r_{DMAEMA} in DMF are both less than one; this scenario highlights a special case in free-radical copolymerization where an azeotrope exists. Copolymerization at the compositional azeotrope results in polymers that have the same composition at any point during the reaction. For HEMA and DMAEMA copolymerization in DMF, the azeotrope occurs at $f_{\text{HEMA}} = F_{\text{HEMA}} = 0.72$.¹⁰

Recently, we described a route to synthesize linear poly(HEMA-*co*-DMAEMA) random copolymers by atom transfer radical polymerization (ATRP).¹⁰ ATRP is a “controlled” free-radical polymerization technique that has been previously utilized to prepare linear poly(HEMA)^{11–17} and poly(DMAEMA)^{16–20} homopolymers and block copolymers.¹⁷ Due to the nature of ATRP, the resulting polymers frequently achieve their target molecular weights and have narrow molecular weight distributions.^{21–23} We extended this concept to making random copolymers of poly(HEMA-*co*-DMAEMA) by ATRP. The copolymerizations were carried out at the compositional azeotrope, so we had control over the molecular weight, molecular weight distribution, and the monomer distribution of the resulting copolymers.¹⁰ Copolymerizations outside the azeotrope, on the other hand, resulted in a significant drift in the average polymer composition. As such, our ability to produce compositionally uniform poly(HEMA-*co*-DMAEMA) had been limited to a single composition at the azeotrope.

In this work, we report r_{HEMA} and r_{DMAEMA} in isopropyl alcohol (IPA), tetrahydrofuran (THF), acetonitrile (ACN), and

* Corresponding author. E-mail: lloo@che.utexas.edu.

dimethyl sulfoxide (DMSO). While Feldermann and co-workers reported that the reactivity ratios determined during certain controlled free-radical copolymerizations, i.e., reverse addition-fragmentation chain transfer polymerizations (RAFT), are different from those determined during conventional free-radical copolymerizations,²⁵ numerous other reports have suggested that the reactivity ratios determined during ATRP are actually comparable to those determined during conventional free-radical copolymerizations.^{26–28} On this basis, we have thus chosen to determine the reactivity ratios of HEMA and DMAEMA during ATRP in polar solvents using a nonlinear least squares statistical method, similar to that proposed by Tidwell and Mortimer.²⁴ In DMSO, r_{HEMA} and r_{DMAEMA} are both near unity, suggesting minimal deviation between the monomer feed and the polymer compositions. Copolymerizations of HEMA and DMAEMA were performed at two different monomer feed compositions ($f_{\text{HEMA}}^0 = 0.25$ and 0.50) by ATRP with little drift in the polymer compositions, and the copolymers achieve their target molecular weights and have narrow molecular weight distributions ($M_w/M_n < 1.11$). The glass transition temperatures of the resulting copolymers increase with increasing HEMA content.

Experimental Section

Materials. 2-Hydroxyethyl methacrylate (Acros, 98%) was vacuum-distilled (40 mTorr, 65 °C) to remove ethylene glycol dimethacrylate¹² and stored at 0 °C prior to use. 2-Dimethylaminoethyl methacrylate (Acros, 98%) was passed through a column of activated basic alumina and stored over molecular sieves at 0 °C prior to use. 1,2,4-Trimethoxybenzene (Acros, 97%), ethyl α -bromoisobutyrate (EBiB, Aldrich, 98%), N,N,N',N'' -pentamethyldiethylenetriamine (PMDETA, Aldrich, 99%), Cu(I)Br (Aldrich, 98%), Cu(I)Cl (Acros, 99%), Cu(II)Cl₂ (Acros, 99%), acetonitrile (Fisher Scientific), dimethyl sulfoxide (extra dry, Fisher Scientific), isopropyl alcohol (Fisher Scientific), and tetrahydrofuran (Fisher Scientific) were used as received.

Copolymerization of Poly(HEMA-co-DMAEMA) for Reactivity Ratio Determination. We carried out the copolymerizations of HEMA and DMAEMA with initial molar monomer feed compositions ranging from $f_{\text{HEMA}}^0 = 0.25$ to $f_{\text{HEMA}}^0 = 0.90$, and with a total monomer:PMDETA:CuBr:EBiB molar ratio of 300:1:1:1. For each copolymerization, 20 g of total monomer feed was used. During a typical copolymerization with a molar monomer feed composition of $f_{\text{HEMA}}^0 = 0.50$, HEMA (9.06 g, 69.6 mmol), DMAEMA (10.9 g, 69.6 mmol), CuBr (66.6 mg, 0.464 mmol), PMDETA (97.0 μL , 0.464 mmol), 4 mL of 1,2,4-trimethoxybenzene (inert; added to reaction medium as an internal GC standard), and 50 mL of DMSO (or 60 mL of ACN, IPA, THF) were added to a 100 mL round-bottom flask equipped with a magnetic stir bar. The flask was sealed with a septum, placed in an oil bath preheated to 45 °C, and purged with N₂ for 30 min. The reaction was initiated by the addition of EBiB (68.8 μL , 0.464 mmol). Positive N₂ pressure was maintained throughout the copolymerizations. Aliquots were drawn at successive time points for a maximum of 24 h for gas chromatography (GC) and ¹H NMR analysis. The aliquots were quenched by cooling to 0 °C and then exposing to air. GC samples were diluted with THF and injected without further purification. The remainder of each aliquot was diluted with THF, passed through activated basic alumina to remove copper salts, and dialyzed against THF (10 mL solution/500 mL THF) for at least 12 h to remove the initial solvent prior to precipitation in hexanes. The aliquots from experiments performed in THF were precipitated directly into hexanes without dialysis. The filtered copolymer was collected and dried at room temperature in a vacuum oven for at least 12 h.

Characterization. We tracked f_{HEMA} during the progression of the copolymerization using an Agilent Technologies 6850 Series II Network GC system containing a poly(dimethylsiloxane) capillary column (12 m \times 200 μm \times 0.25 μm). The eluent was H₂ at a flow rate of 1.5 mL/min. The temperature ramp rate was 10 °C/min.

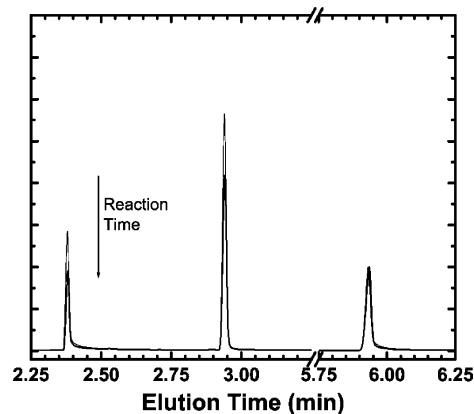


Figure 1. Gas chromatography traces from several time points of a single copolymerization of hydroxyethyl methacrylate (HEMA, 2.4 min) and dimethylaminoethyl methacrylate (DMAEMA, 2.9 min) in tetrahydrofuran at a molar monomer feed composition, f_{HEMA}^0 , of 0.30. The traces are normalized relative to the peak intensity of 1,2,4-trimethoxybenzene (internal standard, 5.9 min). HEMA and DMAEMA peak intensities decrease with increasing reaction time. Monomer conversion was determined from the integrated peak intensities of HEMA and DMAEMA at specific times along the polymerization relative to those in feed.

The flame ionization detector was operated at 300 °C with a H₂ flow rate of 40 mL/min. F_{HEMA} was determined using ¹H NMR spectroscopy in deuterated methanol or deuterated DMSO on a Varian Unity+ 300 MHz NMR spectrometer. We determined the molecular weight distributions by performing gel permeation chromatography (GPC) on a GPC system equipped with a Waters 515 HPLC solvent pump and two PLgel mixed-C columns (5 μm bead size, MW range 200–2 000 000 gmol, Polymer Laboratories, Inc.). The columns were connected in series with an Optilab DSP interferometric refractometer ($\lambda = 690$ nm; Wyatt Technology Corp.) and a multiangle laser light scattering (MALLS) detector ($\lambda = 690$ nm; DAWN-EOS, Wyatt Technology Corp.). The mobile phase was DMF with 0.05 M LiBr (Aldrich) at a flow rate of 1.0 mL/min at 60 °C. LiBr was added to suppress polymer–solvent and polymer–substrate interactions that are typically observed in polymers with ionic functional groups.^{30,31} The absolute molecular weights of the poly(HEMA-co-DMAEMA) copolymers were obtained from GPC data given a dn/dc value of 0.1009, which was previously determined for poly(HEMA-co-DMAEMA) random copolymers with $F_{\text{HEMA}} = 0.72$.¹⁰ Differential scanning calorimetry (DSC) experiments were performed on a Perkin-Elmer DSC 7 equipped with Intracooler II, at a ramp rate of 10 °C/min. Temperature and enthalpy calibrations were performed with indium and zinc standards. The glass transition temperatures were extracted at the midpoint of a step change in heat capacity during the second heat following controlled cooling at a rate of 5 °C/min.

Results and Discussion

Copolymerizations of HEMA and DMAEMA at varying monomer feed compositions were carried out by ATRP in IPA, THF, ACN, and DMSO. Monomer conversion and F_{HEMA} were collected throughout each copolymerization. Representative GC traces collected during a copolymerization in THF with $f_{\text{HEMA}}^0 = 0.30$ at successive time points of 0 h, 2 h, and 6 h are shown in Figure 1. The elution times of HEMA, DMAEMA, and 1,2,4-trimethoxybenzene (nonreactive internal standard) are 2.4, 2.9, and 5.9 min, respectively. The traces for each aliquot are normalized by the peak intensity of 1,2,4-trimethoxybenzene. Since the monomer concentration is directly proportional to the peak intensities, we observe decreases in both the HEMA and the DMAEMA peak intensities with reaction time. To obtain the monomer conversion, we compared the normalized integrated intensities of the monomers with those in the feed, f^0 .

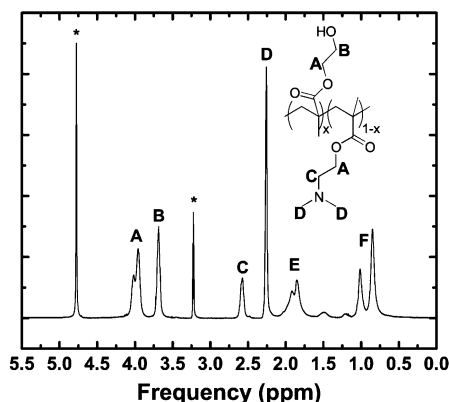


Figure 2. ^1H NMR spectrum of poly(HEMA-*co*-DMAEMA) in deuterated methanol. The integrated areas of peaks A, B, C, and D were used to determine the average polymer composition in each aliquot. The chemical structure of the polymer is included in the inset. * indicates solvent peaks.

The average polymer composition of each aliquot was determined by ^1H NMR. A representative ^1H NMR spectrum of poly(HEMA-*co*-DMAEMA) in deuterated methanol is shown in Figure 2. Peaks A ($\delta = 4.04$ ppm) are characteristic of the α -hydrogens in the ester groups of both HEMA and DMAEMA (2H each); peak B ($\delta = 3.74$ ppm; 2H) is characteristic of the ethyl hydrogens in HEMA; peak C ($\delta = 2.62$ ppm; 2H) is characteristic of the ethyl hydrogens in DMAEMA, peak D ($\delta = 2.30$ ppm; 6H) is characteristic of the hydrogens in the methyl groups of the tertiary amine of DMAEMA, and peaks E and F ($\delta = 0.89$ – 1.94 ppm) are backbone hydrogens. The peak areas of methacrylate (peaks A), HEMA (peak B), and DMAEMA (peaks C and D) were used to determine \bar{F}_{HEMA} .

Assuming a terminal model³¹ for monomer reactivity, the instantaneous polymer composition (F_{HEMA}) during a free-radical copolymerization can be predicted with the Skeist equation (Equation 1), given the reactivity ratios (r_{HEMA} , r_{DMAEMA}) and the instantaneous monomer composition (f_{HEMA}).^{32,33} We note that ^1H NMR, however, provides an average polymer composition (\bar{F}_{HEMA}) rather than an instantaneous copolymer composition. To determine the reactivity ratios, the average polymer composition, as determined by ^1H NMR, must be related to the instantaneous polymer composition in the Skeist equation. We therefore numerically integrated eq 1 over the relevant range of monomer conversion to relate the average polymer composition to the monomer conversion.³¹

$$F_{\text{HEMA}} = \frac{r_{\text{HEMA}}f_{\text{HEMA}}^2 + f_{\text{HEMA}}(1 - f_{\text{HEMA}})}{r_{\text{HEMA}}f_{\text{HEMA}}^2 + r_{\text{DMAEMA}}(1 - f_{\text{HEMA}})^2 + 2f_{\text{HEMA}}(1 - f_{\text{HEMA}})} \quad (1)$$

For each solvent system, the average polymer composition and monomer conversion data were collected from copolymerizations carried out at several monomer feed compositions. Starting with an initial estimate for the reactivity ratios ($r_{\text{HEMA}} = r_{\text{DMAEMA}} = 1$), and given the monomer feed composition and monomer conversion data, theoretical values of the average polymer composition can be determined as a function of monomer conversion. We minimized the sum of the square errors between the theoretical and the experimentally obtained polymer compositions to obtain r_{HEMA} and r_{DMAEMA} . This technique is similar to the nonlinear least-squares regression method proposed by Mortimer and Tidwell.²⁴ But because we integrated the Skeist equation, we were able to use the data

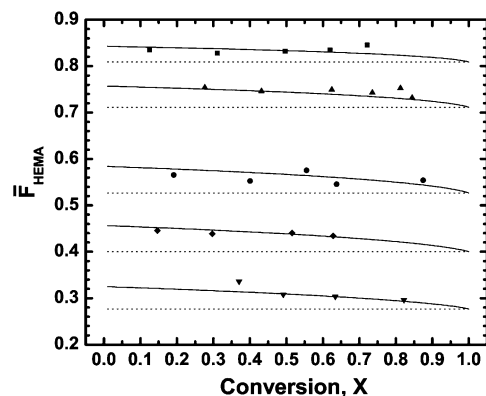


Figure 3. Monomer conversion and average polymer composition data for hydroxyethyl methacrylate (HEMA) and dimethylaminoethyl methacrylate (DMAEMA) copolymerizations in isopropyl alcohol collected from separate atom transfer radical copolymerizations at molar monomer feed compositions, f_{HEMA}^0 , of 0.277 (∇), 0.400 (\blacklozenge), 0.526 (\bullet), 0.711 (\blacktriangle), and 0.808 (\blacksquare). The dotted lines represent the molar monomer feed compositions for each experiment. The solid curves represent the theoretical average polymer composition, predicted by the integrated Skeist equation with regressed reactivity ratios of $r_{\text{HEMA}} = 1.27$ and $r_{\text{DMAEMA}} = 0.800$.

obtained over a wide range of monomer conversions and monomer feed compositions in the regression of the reactivity ratios.³¹ Although it has been suggested that the reactivity ratios obtained by least-squares regression might be dependent on the initial estimates,²⁴ we obtained the same values for r_{HEMA} and r_{DMAEMA} independent of the numerous initial estimates spanning $0.2 < r_{\text{HEMA}}, r_{\text{DMAEMA}} < 10$.

The conversion and polymer composition data for copolymerizations in IPA at several monomer feed compositions are shown in Figure 3. Each point (∇ , \blacklozenge , \bullet , \blacktriangle , \blacksquare) represents an aliquot collected during the copolymerizations. The copolymerizations were performed at monomer feed compositions of $f_{\text{HEMA}}^0 = 0.277$ (∇), 0.400 (\blacklozenge), 0.526 (\bullet), 0.711 (\blacktriangle), and 0.808 (\blacksquare). The dotted lines represent the monomer feed composition for each experiment. The solid curves in Figure 3 represent the theoretical average polymer composition, predicted by the integrated Skeist equation for each copolymerization. If there is no deviation between the average polymer composition and the monomer feed composition (as in the case when $r_{\text{HEMA}} = r_{\text{DMAEMA}} = 1$), the solid curves should coincide with the dashed lines. Using least-squares regression, r_{HEMA} and r_{DMAEMA} were determined to be 1.27 and 0.800 in IPA, respectively.

As a means of comparison, the reactivity ratios were also calculated according to the methods proposed by Fineman and Ross,³⁴ and Kelen and Tudos.³⁵ In these calculations, we used only the data obtained at low conversion (i.e., the first data points during each of the copolymerizations in Figure 3). The reactivity ratios calculated by all three methods are shown in Table 1. The values obtained using the methods of Fineman and Ross, and Kelen and Tudos, are similar to those determined by least-squares regression. We believe that the least-squares regression technique is the most reliable, since more data (obtained at higher conversions and at various monomer feed compositions) were used to determine r_{HEMA} and r_{DMAEMA} .

We also determined r_{HEMA} and r_{DMAEMA} in THF, ACN, and DMSO in a similar fashion; the calculated reactivity ratios are summarized in Table 1. To demonstrate the effect of solvent selection on r_{HEMA} and r_{DMAEMA} , we have plotted the least-squares regressed values in Figure 4, along with previously reported values for r_{HEMA} and r_{DMAEMA} in the bulk,⁸ in water,⁹ and in DMF.⁹ We have drawn 95% joint confidence regions around the reactivity ratios in IPA, THF, ACN, and DMSO, as

Table 1. Solubility Parameters (δ) of Solvents and Reactivity Ratios (r_{HEMA} , r_{DMAEMA}) of Hydroxyethyl Methacrylate (HEMA) and Dimethylaminoethyl Methacrylate (DMAEMA) Calculated by Various Methods from Atom Transfer Radical Copolymerizations

solvent	solubility parameter: ⁴¹ δ (cal/cm ³) ^{1/2}	solubility parameter difference: $(\delta - \delta_{\text{HEMA}})^2$	least-squares regression		Fineman and Ross ³⁴		Kelen and Tudos ³⁵	
			r_{HEMA}	r_{DMAEMA}	r_{HEMA}	r_{DMAEMA}	r_{HEMA}	r_{DMAEMA}
isopropyl alcohol	11.5	2.9	1.27	0.800	1.19	0.783	1.18	0.767
tetrahydrofuran	9.1	17	1.46	0.926	1.52	0.857	1.49	0.844
acetonitrile	11.9	1.7	1.01	0.641	1.02	0.681	1.04	0.699
dimethyl sulfoxide	14.5	1.7	1.08	1.12	0.976	1.02	1.05	1.09

determined using the method of Tidwell and Mortimer.²⁴ We have also plotted the Skeist equation (eq 1), given the calculated r_{HEMA} and r_{DMAEMA} , for the copolymerization of HEMA and DMAEMA in IPA, THF, ACN, and DMSO in Figures 5, parts a, b, c, and d, respectively (solid curves). The dashed line in each plot is the 45° line that represents the case of $F_{\text{HEMA}} = f_{\text{HEMA}}$. The Skeist equation should predict exactly this line when both reactivity ratios are unity. The difference between the solid curve and the dashed line thus represents deviations between the instantaneous monomer composition and the instantaneous polymer composition. In IPA ($r_{\text{HEMA}} = 1.27$ and $r_{\text{DMAEMA}} = 0.800$; Figure 5a) and in THF ($r_{\text{HEMA}} = 1.46$ and $r_{\text{DMAEMA}} = 0.926$; Figure 5b), r_{HEMA} is greater than unity, whereas r_{DMAEMA} is less than unity. This suggests that the addition of HEMA is favored over the addition of DMAEMA to a growing polymer chain. A gradient copolymer that is initially enhanced in HEMA, rather than a random copolymer, thus results during polymerizations in IPA and THF. Given the calculated reactivity ratios, we predict a greater than 4% deviation between the instantaneous monomer composition and the instantaneous polymer composition over 50% of the entire composition range when copolymerizations take place in either IPA or THF. This deviation is apparent in Figures 5a and 5b, where considerable differences between F_{HEMA} and f_{HEMA} are observed in both solvents. The calculated r_{HEMA} and r_{DMAEMA} in ACN are 1.01 and 0.641, respectively. As shown in Figure 5c, HEMA is preferentially added at low f_{HEMA} . At high f_{HEMA} (~0.95–0.99) the solid curve coincides with the 45° line, suggesting minimal deviation between f_{HEMA} and F_{HEMA} . Our 95% confidence interval does not preclude the presence of an azeotrope at $f_{\text{HEMA}} > 0.95$.

The calculated reactivity ratios in DMSO are $r_{\text{HEMA}} = 1.08$ and $r_{\text{DMAEMA}} = 1.12$. The Skeist equation predicts an azeotropic composition in DMSO at $f_{\text{HEMA}} = 0.609$. In general, however, the reactivity ratios in DMSO are both close to unity. There is

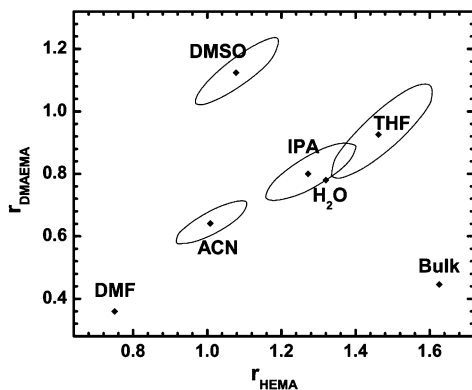


Figure 4. Reactivity ratios of hydroxyethyl methacrylate (r_{HEMA} , x-axis) and dimethylaminoethyl methacrylate (r_{DMAEMA} , y-axis) determined from atom transfer radical copolymerizations, along with 95% joint confidence intervals (ellipses), for isopropyl alcohol (IPA), tetrahydrofuran (THF), acetonitrile (ACN), and dimethyl sulfoxide (DMSO). Previously reported reactivity ratios in the bulk,⁸ in water (H₂O),⁹ and in *N,N*-dimethylformamide (DMF)⁹ are also shown.

therefore very little deviation between the instantaneous monomer composition and the instantaneous polymer composition over the entire range of f_{HEMA} , as shown in Figure 5d. We carried out two additional copolymerizations in DMSO at $f_{\text{HEMA}}^0 = 0.25$ and 0.50. In both cases, the average polymer composition during the polymerization is maintained at the monomer feed composition.

The role of solvent on the reactivity ratios of polar monomers is qualitatively described by the bootstrap effect,^{36,37} which surmises polarity-induced differences in the local monomer concentration.^{38,39} This model, however, does not provide a prescriptive guide to the selection of the appropriate solvent for producing random copolymers of uniform compositions. During the copolymerization of HEMA and DMAEMA, we noted an interesting correlation between the solubility parameter of the solvent and the extracted reactivity ratios. In particular, we observe that $r_{\text{HEMA}} \approx 1$ when the solubility parameter of the solvent (δ) closely matches the solubility parameter of poly(HEMA), $\delta_{\text{HEMA}} = 13.2$ (cal/cm³)^{1/2}.⁴⁰ For discussion, we have listed the solubility parameters of the solvents,⁴¹ along with the square of the solubility parameter difference, $(\delta - \delta_{\text{HEMA}})^2$, which is proportional to the contact energy of the solvent and poly(HEMA),⁴² in Table 1. We observe that $r_{\text{HEMA}} \approx 1$ when $(\delta - \delta_{\text{HEMA}})^2$ is small (<2). With increasing $(\delta - \delta_{\text{HEMA}})^2$, however, r_{HEMA} increases. This trend is consistent with what had been proposed by the bootstrap effect.^{36,37} When the solvent–polymer contact energy is high, the local environment of the growing chain is likely enhanced in HEMA monomer. The propensity for the growing radical to add a HEMA monomer is thus high ($r_{\text{HEMA}} > 1$). On the other hand, when the solvent–polymer contact energy is minimal, the local environment is not enhanced in HEMA, so r_{HEMA} is approximately 1. Our discussion here does not take DMAEMA into account. While we acknowledge that the presence of DMAEMA necessarily changes the local environment, we were not able to find the solubility parameter of DMAEMA in the literature for this comparison. But we speculate the effect to be small given that DMAEMA is not capable of hydrogen bonding (or any other specific interactions), except in water where the tertiary amine group can be quarternized under acidic conditions.^{4,8}

To demonstrate the versatility of DMSO as a copolymerization medium for poly(HEMA-*co*-DMAEMA), we carried out the copolymerizations of HEMA and DMAEMA in DMSO at $f_{\text{HEMA}}^0 = 0.25$ and $f_{\text{HEMA}}^0 = 0.50$ by ATRP. It has been previously reported that DMSO can coordinate with both Cu(I) and Cu(II), and that these interactions can complicate the polymerization kinetics and the controllability of reactions performed in DMSO.¹⁶ To improve control over our copolymerizations, we used a mixed halide system consisting of a bromine initiator and chloride catalyst¹⁰ instead of just using copper bromide. A mixed halide system has been previously demonstrated to promote faster initiation and slower propagation.^{10,43,44} We also performed the copolymerizations with a low concentration of Cu(I)Cl (1:10 molar, relative to EBIB) and a

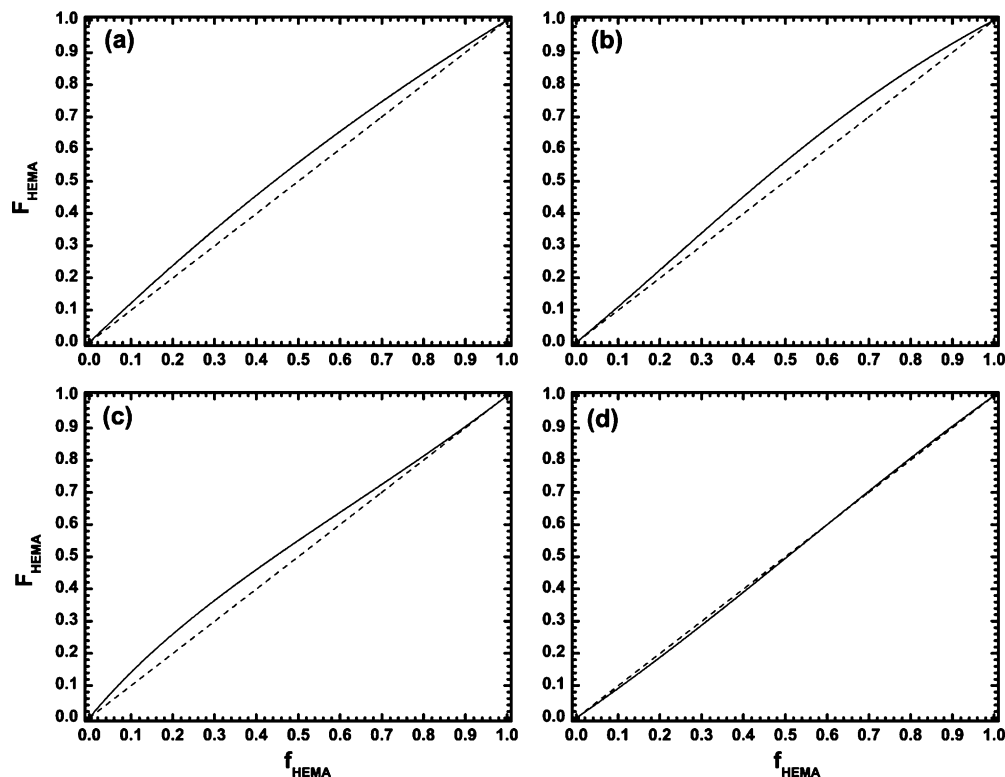


Figure 5. The Skeist equation for the atom transfer radical copolymerization of hydroxyethyl methacrylate (HEMA) and dimethylaminoethyl methacrylate (DMAEMA) in (a) isopropyl alcohol, (b) tetrahydrofuran, (c) acetonitrile, and (d) dimethyl sulfoxide, as predicted from the reactivity ratios in each solvent. The dashed line in each graph corresponds to the 45° line where the instantaneous polymer composition is equal to the instantaneous monomer composition ($F_{\text{HEMA}} = f_{\text{HEMA}}$), which occurs when both reactivity ratios are unity.

high concentration of Cu(II)Cl_2 (1.2:1 molar, relative to EBIB) to suppress any early termination reactions during the copolymerization.⁴⁵

The kinetics of poly(HEMA-*co*-DMAEMA) copolymerizations by ATRP in DMSO do not follow the classical first order kinetics attributed to living polymerizations. As we have previously observed for copolymerizations of HEMA and DMAEMA in DMF,¹⁰ these copolymerizations follow a $t^{1/3}$ model proposed by Snijder and co-workers.⁴⁶ The $t^{1/3}$ model is attributed to the loss of Cu(II) above a ceiling concentration. In general, the copolymerizations are faster with increasing f_{HEMA}^0 . To quantify, we calculated the rate coefficient of propagation, k_p , for copolymerizations in DMSO at $f_{\text{HEMA}}^0 = 0.25$ and $f_{\text{HEMA}}^0 = 0.50$, assuming that the ATRP equilibrium constant, K_{eq} , and the ceiling Cu(II) concentration, $[\text{Cu(II)}]_c$, are independent of the monomer feed composition. Under these assumptions, the rate coefficient of propagation at $f_{\text{HEMA}}^0 = 0.50$ is 1.5 times greater than that at $f_{\text{HEMA}}^0 = 0.25$. It has been previously observed that the rate of polymerization of HEMA is considerably faster than the rate of polymerization of DMAEMA, when polymerizations take place under similar conditions.¹⁷ It is therefore not surprising that the overall rate of copolymerization is related to the feed composition and is enhanced with increasing HEMA in the monomer feed.

The copolymers collected during the copolymerizations in DMSO with $f_{\text{HEMA}}^0 = 0.25$ and $f_{\text{HEMA}}^0 = 0.50$ were analyzed by ^1H NMR, and little deviation (<1.5 mol %) between the initial monomer composition and the average polymer composition of each aliquot was observed. The copolymers were also analyzed by GPC with DMF (+ 0.05 M LiBr) as the eluent. All the GPC traces are narrow and monomodal; the peaks shift to smaller elution volumes with increasing monomer conversion. The extracted molecular weight distributions for the copolymers are plotted as a function of total monomer conversion in Figure

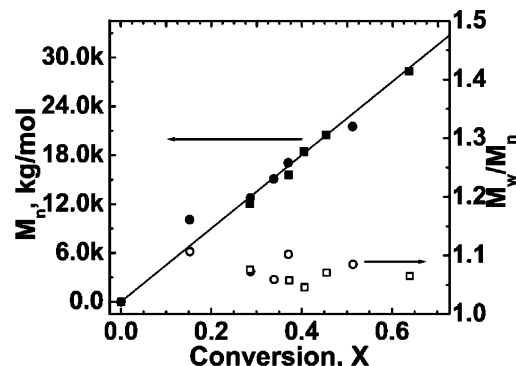


Figure 6. The molecular weight of poly(HEMA-*co*-DMAEMA) as a function of monomer conversion during atom transfer radical copolymerizations in dimethyl sulfoxide at molar monomer feed compositions, f_{HEMA}^0 , of 0.25 (●,○) and 0.50 (■,□). The absolute number-average molecular weight (M_n ; ■,●) is plotted on the left axis, and the overall molecular weight distribution (M_w/M_n ; □,○) is plotted on the right axis. The solid line represents the theoretical molecular weight, as predicted from the monomer-to-initiator ratio.

6. The molecular weight distributions remained narrow (<1.11), even at high monomer conversions ($X = 0.637$). The molecular weight distributions are generally narrower than those we previously reported for copolymerizations in DMF.¹⁰ We speculate that we now have better control over the copolymerization with a reduction in Cu(I) concentration and an increase in Cu(II) concentration.

The absolute number-average molecular weights for copolymers are also plotted in Figure 6. During both copolymerizations, the molecular weights increased linearly with total monomer conversion. For reference, we have also plotted the theoretical molecular weight, as predicted by the monomer-to-initiator ratio in Figure 6 (solid line). The molecular weights appear to fall on the theoretical molecular weight line, which points to the

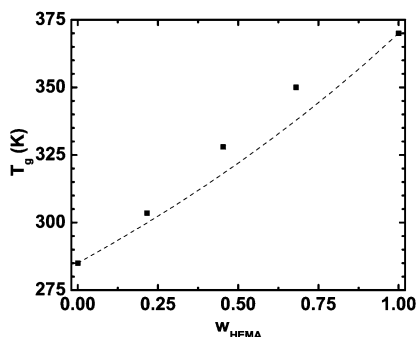


Figure 7. The glass transition temperatures of poly(HEMA), poly(DMAEMA), and poly(HEMA-*co*-DMAEMA) random copolymers. The dashed curve represents the Fox equation given the glass transition temperatures of the two homopolymers.

“livingness” of this polymerization.²¹ Previously, we observed deviations between the theoretical and experimental molecular weights during copolymerizations of HEMA and DMAEMA in DMF. This observation was largely independent of the type of initiator (polystyrene macroinitiator or EB/B) and the monomer to initiator molar ratio,¹⁰ and we attributed the molecular weight deviation away from the theoretical quantity to low initiation efficiency and early termination of the free radicals. By decreasing the Cu(I) concentration and correspondingly increasing the Cu(II) concentration, it appears we have successfully suppressed the early termination reactions.

We measured the glass transition temperatures (T_g) of poly(HEMA-*co*-DMAEMA) synthesized by ATRP in DMSO by DSC. The samples were heated twice; the first heat provided a uniform thermal contact between the sample and the pan, and we only extracted the glass transition temperature from the second heat. The DSC thermograms of each copolymer show a single-step change in enthalpy indicating a glass transition. We also determined the glass transition temperatures of poly(DMAEMA) and poly(HEMA) homopolymers. All the extracted T_g s are plotted against the weight fraction of HEMA, w_{HEMA} , within the random copolymer in Figure 7. We have also included the T_g of poly(HEMA-*co*-DMAEMA) with average polymer composition $F_{\text{HEMA}} = 0.72$, which was synthesized previously in DMF.¹⁰ The glass transition temperature increases with increasing HEMA content, and the trend appears to be qualitatively described by the Fox equation (dashed line; based on eq 2):⁴⁷

$$\frac{1}{T_g} = \frac{w_{\text{HEMA}}}{T_{g,\text{HEMA}}} + \frac{1 - w_{\text{HEMA}}}{T_{g,\text{DMAEMA}}} \quad (2)$$

That the Fox equation satisfactorily describes the increase in T_g we observe in our polymers is unexpected, given that HEMA is capable of hydrogen bonding.⁸ Contrary to what has been proposed for HEMA-containing systems,⁸ our observations suggest that the specific interactions do not dominate the physical properties in our copolymers.

Conclusions

We have determined the reactivity ratios of HEMA and DMAEMA in IPA, THF, ACN, and DMSO. The reactivity ratios of HEMA and DMAEMA are highly solvent dependent; the average polymer composition deviates from the monomer feed composition significantly when the copolymerization is carried out in IPA, THF, and ACN. In DMSO, however, both the reactivity ratios of HEMA and DMAEMA are near unity, so the average polymer composition is that of the monomer

feed composition over the entire compositional range. Poly(HEMA-*co*-DMAEMA) copolymers were synthesized by ATRP in DMSO with uniform compositions, predictable molecular weights, and narrow molecular weight distributions ($M_w/M_n < 1.11$). The glass transition temperatures of the resulting copolymers increase with increasing HEMA content.

Acknowledgment. This work is funded by the National Science Foundation (NSF CAREER DMR-0348339) and a Camille and Henry Dreyfus New Faculty Award. Support from the Keck Foundation, the Welch Foundation, and Texas Materials Institute are also gratefully acknowledged. R.L.T. acknowledges the University Cooperative Society for an undergraduate research fellowship and the NSF for an REU supplement. K.B.G. acknowledges the NSF for a graduate fellowship. We thank Dr. Chris Bielawski and Dan Coady for assistance with GC measurements.

References and Notes

- (1) Kroupova, J.; Horak, D.; Pachernik, J.; Dvorak, P.; Slouf, M. *J. Biomed. Mater. Res., Part B: Appl. Biomater.* **2006**, *76B*, 315–325.
- (2) Willcox, M. D. P.; Harmis, N.; Cowell, B. A.; Williams, T.; Holden, B. A. *Biomaterials* **2001**, *22*, 3235–3247.
- (3) Abraham, S.; Brahim, S.; Ishihara, K.; Guiseppi-Elie, A. *Biomaterials* **2005**, *26*, 4767–4778.
- (4) Van de Wetering, P.; Moret, E. E.; Schuurmans-Nieuwenbroek, N. M. E.; Van Steenberg, M. J.; Hennink, W. E. *Bioconjugate Chem.* **1999**, *10*, 589–597.
- (5) Brahim, S.; Narinesingh, D.; Guiseppi-Elie, A. *Biomacromolecules* **2003**, *4*, 1224–1231.
- (6) Brahim, S.; Narinesingh, D.; Guiseppi-Elie, A. *Biomacromolecules* **2003**, *4*, 497–503.
- (7) Trifitaridou, A. I.; Hadjiyannakou, S. C.; Vamvakaki, M.; Patrickios, C. S. *Macromolecules* **2002**, *35*, 2506–2513.
- (8) Martin-Gomis, L.; Cuervo-Rodriguez, R.; Fernandez-Monreal, M. C.; Madruga, E. L.; Fernandez-Garcia, M. *J. Polym. Sci., Part A: Polym. Chem.* **2003**, *41*, 2659–2666.
- (9) Mathew-Krotz, J.; Mahadevan, V. *Macromol. Chem. Phys.* **1997**, *198*, 1597–1604.
- (10) Guice, K. B.; Loo, Y.-L. *Macromolecules* **2006**, *39*, 2474–2480.
- (11) Tsarevsky, N. V.; Pintauer, T.; Matyjaszewski, K. *Macromolecules* **2004**, *37*, 9768–9778.
- (12) Weaver, J. V. M.; Bannister, I.; Robinson, K. L.; Bories-Azeau, X.; Armes, S. P.; Smallridge, M.; McKenna, P. *Macromolecules* **2004**, *37*, 2395–2403.
- (13) Robinson, K. L.; Khan, M. A.; de Banez, M. V.; Wang, X. S.; Armes, S. P. *Macromolecules* **2001**, *34*, 3155–3158.
- (14) Beers, K. L.; Boo, S.; Gaynor, S. G.; Matyjaszewski, K. *Macromolecules* **1999**, *32*, 5772–5776.
- (15) Simal, F.; Demonceau, A.; Noels, A. F. *Angew. Chem., Int. Ed.* **1999**, *38*, 538–540.
- (16) Monge, S.; Darcos, V.; Haddleton, D. M. *J. Polym. Sci., Part A: Polym. Chem.* **2004**, *42*, 6299–6308.
- (17) Jin, X.; Shen, Y.; Zhu, S. *Macromol. Mater. Eng.* **2003**, *288*, 925–935.
- (18) Lee, S. B.; Russell, A. J.; Matyjaszewski, K. *Biomacromolecules* **2003**, *4*, 1386–1393.
- (19) Mao, B.; Gan, L.-H.; Gan, Y.-Y.; Li, X.; Ravi, P.; Tam, K.-C. *J. Polym. Sci., Part A: Polym. Chem.* **2004**, *42*, 5161–5169.
- (20) Zhang, X.; Xia, J.; Matyjaszewski, K. *Macromolecules* **1998**, *31*, 5167–5169.
- (21) Matyjaszewski, K.; Xia, J. *Chem. Rev.* **2001**, *101*, 2921–2990.
- (22) Buchholz, T. L.; Loo, Y.-L. *Macromolecules* **2006**, *39*, 6075–6080.
- (23) Smith, Q.; Huang, J.; Matyjaszewski, K.; Loo, Y.-L. *Macromolecules* **2005**, *38*, 5581–5586.
- (24) Tidwell, P. W.; Mortimer, G. A. *J. Polym. Sci., Part A: Gen. Papers* **1965**, *3*, 369–387.
- (25) Feldermann, A.; Toy, A. A.; Phan, H.; Stenzel, M. H.; Davis, T. P.; Barner-Kowollik, C. *Polymer* **2004**, *45*, 3997–4007.
- (26) Braunecker, W. A.; Tsarevsky, N. V.; Pintauer, T.; Gil, R. R.; Matyjaszewski, K. *Macromolecules* **2005**, *38*, 4081–4088.
- (27) Roos, S. G.; Müller, A. H. E.; Matyjaszewski, K. *Macromolecules* **1999**, *32*, 8331–8335.
- (28) Haddleton, D. M.; Crossman, M. C.; Hunt, K. H.; Topping, C.; Waterson, C.; Suddaby, K. G. *Macromolecules* **1997**, *30*, 3992–3998.
- (29) Dias, M. L.; Mano, E. B.; Azuma, C. *Eur. Polym. J.* **1997**, *33*, 559–564.

- (30) Dubin, P. L.; Koontz, S.; Wright, K. L., III. *J. Polym. Sci., Polym. Chem. Ed.* **1977**, *15*, 2047–2057.
- (31) Czerwinski, W. K. *Polymer* **1997**, *39*, 183–187.
- (32) Skeist, I. *J. Am. Chem. Soc.* **1946**, *68*, 1781–1784.
- (33) Odian, G. *Principles of Polymerization*, 4th ed.; Wiley-Interscience: New York, 2004.
- (34) Fineman, M.; Ross, S. D. *J. Polym. Sci.* **1950**, *5*, 259–262.
- (35) Kelen, T.; Tudos, F. *J. Macromol. Sci., Chem.* **1975**, *A9*, 1–27.
- (36) Klumperman, B.; O'Driscoll, K. F. *Polymer* **1993**, *34*, 1032–1037.
- (37) Klumperman, B.; Kraeger, I. R. *Macromolecules* **1994**, *27*, 1529–1534.
- (38) Cowie, J. M. G.; McEwen, I. J.; Yule, D. J. *Eur. Polym. J.* **2000**, *36*, 1795–1803.
- (39) Fernandez-Monreal, C.; Martinez, G.; Sanchez-Chaves, M.; Madruga, E. L. *J. Polym. Sci., Part A: Polym. Chem.* **2001**, *39*, 2043–2048.
- (40) Caykara, T.; Ozyurek, C.; Kantoglu, O.; Guven, O. *J. Polym. Sci., Part B: Polym. Phys.* **2002**, *40*, 1995–2003.
- (41) *Polymer Handbook*, 4th ed.; Brandrup, J.; Immergut, E. H.; Grulke, E. A., Eds.; Wiley-Interscience: New York, 1999.
- (42) Young, R. J.; Lovell, P. A. *Introduction to Polymers*, 2nd ed.; Chapman & Hall: London, 1991.
- (43) Matyjaszewski, K.; Shipp, D. A.; Wang, J.-L.; Grimaud, T.; Patten, T. E. *Macromolecules* **1998**, *31*, 6836–6840.
- (44) Schellekens, M. A. J.; de Wit, F.; Klumperman, B. *Macromolecules* **2001**, *34*, 7961–7966.
- (45) Matyjaszewski, K.; Xia, J. Fundamentals of Atom Transfer Radical Polymerization. In *Handbook of Radical Polymerization*; Matyjaszewski, K.; Davis, T. P., Eds. Wiley-Interscience: New York, 2002; pp 523–628.
- (46) Snijder, A.; Klumperman, B.; van der Linde, R. *Macromolecules* **2002**, *35*, 4785–4790.
- (47) Fox, T. G. *Bull. Am. Phys. Soc.* **1956**, *1*, 123.

MA061650B